catalysts

MDPI

Article

Mineralization of Lipase from *Thermomyces lanuginosus* Immobilized on Methacrylate Beads Bearing Octadecyl Groups to Improve Enzyme Features

José R. Guimarães [1,2], Diego Carballares [1], Javier Rocha-Martin [3], Paulo W. Tardioli [2,*] and Roberto Fernandez-Lafuente [1,4,*]

[1] Departamento de Biocatálisis, ICP-CSIC, Campus UAM-CSIC, 28049 Madrid, Spain
[2] Graduate Program in Chemical Engineering (PPGEQ), Laboratory of Enzyme Technologies (LabEnz), Department of Chemical Engineering, Federal University of São Carlos (DEQ/UFSCar), Rod. Washington Luís, km 235, São Carlos 13565-905, SP, Brazil
[3] Department of Biochemistry and Molecular Biology, Faculty of Biology, Complutense University of Madrid, José Antonio Novais 12, 28040 Madrid, Spain
[4] Center of Excellence in Bionanoscience Research, Member of the External Scientific Advisory Board, King Abdulaziz University, Jeddah 21589, Saudi Arabia
* Correspondence: pwtardioli@ufscar.br (P.W.T.); rfl@icp.csic.es (R.F.-L.); Tel.: +55-16-3351-9362 (P.W.T.); +34-9159-4804 (R.F.-L.)

Abstract: Lipase from *Thermomyces lanuginosus* (TLL) has been immobilized on Purolite Lifetech® ECR8806F (viz. methacrylate macroporous resin containing octadecyl groups, designated as Purolite C18-TLL), and the enzyme performance has been compared to that of the enzyme immobilized on octyl-agarose, designated as agarose C8-TLL. The hydrolytic activity versus *p*-nitrophenol butyrate decreased significantly, and to a lower extent versus *S*-methyl mandelate (more than twofold), while versus triacetin and *R*-methyl mandelate, the enzyme activity was higher for the biocatalyst prepared using Purolite C18 (up to almost five-fold). Regarding the enzyme stability, Purolite C18-TLL was significantly more stable than the agarose C8-TLL. Next, the biocatalysts were mineralized using zinc, copper or cobalt phosphates. Mineralization increased the hydrolytic activity of Purolite C18-TLL versus triacetin and *R*-methyl mandelate, while this activity decreased very significantly versus the *S*-isomer, while the effects using agarose C8-TLL were more diverse (hydrolytic activity increase or decrease was dependent on the metal and substrate). The zinc salt treatment increased the stability of both biocatalysts, but with a lower impact for Purolite C18-TLL than for agarose-C8-TLL. On the contrary, the copper and cobalt salt treatments decreased enzyme stability, but more intensively using Purolite C18-TLL. The results show that even using enzymes immobilized following the same strategy, the differences in the enzyme conformation cause mineralization to have diverse effects on enzyme stability, hydrolytic activity, and specificity.

Keywords: lipase immobilization; immobilization on Purolite C18; mineralization of immobilized lipase; modulation of lipase hydrolytic activity; lipase stabilization

check for updates

Citation: Guimarães, J.R.; Carballares, D.; Rocha-Martin, J.; Tardioli, P.W.; Fernandez-Lafuente, R. Mineralization of Lipase from *Thermomyces lanuginosus* Immobilized on Methacrylate Beads Bearing Octadecyl Groups to Improve Enzyme Features. *Catalysts* **2022**, *12*, 1552. https://doi.org/10.3390/catal12121552

Academic Editor: Chiching Hwang

Received: 2 November 2022
Accepted: 29 November 2022
Published: 1 December 2022

Publisher's Note: MDPI stays neutral with regard to jurisdictional claims in published maps and institutional affiliations.

Copyright: © 2022 by the authors. Licensee MDPI, Basel, Switzerland. This article is an open access article distributed under the terms and conditions of the Creative Commons Attribution (CC BY) license (https://creativecommons.org/licenses/by/4.0/).

1. Introduction

The lipase from *Thermomyces lanuginosus* (TLL) is among the most utilized lipases worldwide due to its high stability and the possibility of using it as a catalyst in many different reactions [1]. The immobilization of this enzyme has shown to be a way to further improve the enzyme's features [1].

Enzyme immobilization protocols can be designed to be coupled to enzyme purification [2], and enzyme stability may be improved by different paths (e.g., multipoint covalent attachment, the generation of favorable environments, etc.) [3]. Furthermore, enzyme inhibition, selectivity and specificity may be tuned in quite a random way through enzyme immobilization. This makes it highly recommendable to have an extensive library

of biocatalysts of the same enzyme in order to have one biocatalyst with suitable features for a specific process [4]. This makes enzyme immobilization a critical point nowadays in the development of a biocatalyst [5–10], although to take full advantage of the technique, many aspects need to be considered, and some points require further research to have full control of the process [11]. All these benefits may also be achieved when immobilizing TLL.

Immobilization of enzymes may be achieved using very diverse strategies. They can be immobilized on preexisting supports, with the advantages that this can have: the physical properties of the final biocatalysts will not depend on the enzyme, it is possible to select the mechanical properties of the biocatalyst as a function of the reactor, and it is possible to control the activation degree in the support without affecting the final mechanical properties of the biocatalyst, etc. [9]. They have also some problems [11]; the most obvious is the necessity of finding a support supplier and the costs of the support (including acquisition, storage, activation, and discarding costs). Moreover, the enzyme will interact with only a percentage of its surface with the support (except using supports activated with polymers, or if the enzyme is later modified with a polymer, (e.g., polyethyleneimine)) [12]. The other alternative is the immobilization forming ex novo supports. Examples of this strategy are the production of enzyme co-polymers [13,14], the trapping of the enzymes (e.g., in alginate beads [15–17] or sol-gels [18–20]), cross-linked enzyme crystals [21–23], cross-linked enzyme aggregates [24–27], crystals coated with proteins [28–31], or nanoflowers [32–34]). These methods do not require a support, but require other compounds that can be relatively expensive in some cases (e.g., protein or polymer feeders). One advantage that is common to all of them is that the entire enzyme surface may be involved in the immobilization; thus, in general, they can be very useful to stabilize complex multimeric enzymes where the first inactivation step was the subunit dissociation [35]. In some instances, such as the case of metal-organic framework (MOFs), the solid may be prepared and then immobilize the enzyme (that is, using a pre-existing solid), or may be prepared in the presence of the enzyme forming the solid while the enzyme is immobilized at the same time (that is, forming an ex novo solid) [36–39].

Nanoflowers of lipases have been prepared in many instances, and, in certain cases, this enzyme mineralization promotes improvements in its catalytic activity and/or stability [40–50]. However, their small size and mechanical fragility make these biocatalysts difficult to implement in industry. This has been solved by using magnetic materials to facilitate their handling [51–58], or by trapping the nanoflowers in larger and more resistant materials [59,60]. In this sense, recently, it has been proposed that the mineralization of previously immobilized enzymes can couple the advantages of enzyme mineralization and enzyme immobilization on pre-existing supports, although the formation of proper nanoflowers cannot be observed [61,62]. These previous studies also showed that the enzyme conformation can play a critical role on the final effects of the mineralization [63,64]. This effect of protein conformation on the enzyme mineralization has been previously indicated by other authors using free enzymes [65]; very recently, another paper has shown that the crystals formed using a protein and 2-methylimidazole and zinc acetate metal–organic frameworks strongly depended on the protein structure and its molecular modifications [66].

As a general method of lipases' immobilization (and of TLL in particular), the immobilization of the enzyme via interfacial activation on hydrophobic supports is advantageous, as it permits having the open and monomeric form of the lipases in one step, improving their stability and purifying the lipases [67,68]. It has been shown that the exact nature of the hydrophobic support (internal geometry, hydrophobicity, etc.) can greatly alter lipase functional properties, suggesting that the flexibility of the active center of the lipase can yield different lipase "open" forms [69–73]. The previous studies on the effects of immobilized enzyme mineralization were performed utilizing octyl agarose (named agarose C8 in this paper). In this new research effort, we have utilized methacrylate beads bearing octadecyl groups (named Purolite C18 in this paper) to immobilize the enzyme. Together with different groups in the supports (octyl versus octadecyl), agarose is formed

by trunks of agarose [74], while the metacrylated beads are prepared by using porogenic agents during polymerization; thus, the internal geometry of the surfaces will be different: concave or convex. Based on the previous literature and the enzyme performance, we can assume that although the enzyme will be immobilized via interfacial activation on both agarose C8 and methacrylate beads bearing octadecyl, its final conformation may be different. TLL immobilized on a similar support has proved to be a very efficient biocatalyst in the production of biodiesel [75–77] thus, the tuning of the features of this biocatalyst via mineralization may be of great interest. This support has as one main difference compared to the previous one: a larger particle size. Therefore, in this paper we have analyzed the possibility of tuning (and improving) the hydrolytic activity (versus different substrates) and stability of TLL immobilized on this support, as a first step to their utilization in biodiesel production, comparing the effects with those described using agarose C8.

2. Results

2.1. Preparation of the Immobilized and Chemically Modified TLL

Figure 1 shows the immobilization courses of the enzyme immobilized on agarose C8 and Purolite C18. The hydrolytic activity of the enzyme in the presence of inert agarose beads remains unchanged throughout the immobilization process (that is, the enzyme is not immobilized on the inert agarose and remains fully active, as shown in the reference line of the figures). As expected [61,63,67,69], using agarose C8, immobilization was very rapid, with a small increase in immobilization yield from 0.5 to 2 h (around 55% of the enzyme became immobilized) (around 11 mg/g). Using Purolite C18, immobilization was slower, perhaps due to the larger particle size (300–710 μm), which makes diffusion of the enzyme more problematic [78]. After 2 h, around 45% of the enzyme hydrolytic activity was immobilized (9 mg/g of support). Hydrolytic activity versus *p*-NPB of the immobilized enzyme is not included, as in the case of the Purolite C18 the values are almost 0.

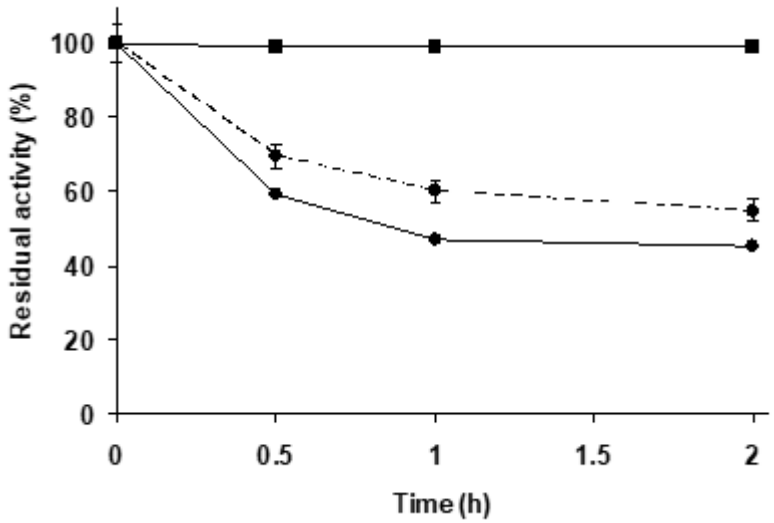

Figure 1. Immobilization course of TLL over agarose C8 beads (solid line) and Purolite C 18 (pointed line) beads offering 20 mg of enzyme per g of support (10 mL of 2 mg enzyme/mL per g of support). Squares: reference (the enzyme under the same conditions of the immobilization suspension but using inert agarose beads) and circles: supernatant. Other specifications are described in Methods.

Table 1 shows the hydrolytic activities of both biocatalysts versus triacetin and both isomers of methyl mandelate. The hydrolytic activity versus *p*-NPB was almost 0 using Purolite C18-TLL. Moreover, the amount of immobilized enzyme was slightly lower using Purolite C18 (9 mg/g) compared to agarose C8 (11 mg/g) (see Figure 1). However, the hydrolytic activity of Purolite C18-TLL was more than 4-fold higher than that of the agarose C8 preparation using the triacetin assay. In the case of methyl mandelate, the effects of

the support depended on the enantiomer used. While the hydrolytic activity versus the *R*-isomer increased using Purolite C18-TLL (by almost 1.7-fold), the hydrolytic activity versus the S-isomer was more than two times higher using agarose C8-TLL. As a result, the hydrolytic activities ratio with these isomers increased from 1.9 using agarose C8-TLL to 7.3 using Purolite C18-TLL. Considering that the diffusional and steric restrictions must be identical for both isomers, this suggests that the differences in hydrolytic activities are really related to different enzyme conformations [4]. Due to this, the immobilization on different supports produced biocatalysts with very different hydrolytic activities and specificities.

Table 1. Activity of the prepared biocatalysts in the hydrolysis of different substrates under the defined conditions. Experiments were conducted as described in Methods.

Biocatalysts	Activity (U/g)		
	Substrate		
	Triacetin	*R*-Mandelate	*S*-Mandelate
Agarose C8-TLL	115.7 ± 5.9	1.3 ± 0.1	0.70 ± 0.05
Purolite C18-TLL	548.7 ± 25.9	2.2 ± 0.1	0.30 ± 0.02

Figure 2 shows that TLL immobilized on Purolite C18 was significantly more stable than the enzyme immobilized on agarose C8 (following the hydrolytic activity with triacetin), which is already considered as a very stable biocatalyst [67,68]. Purolite C18-TLL seemed to offer some advantages in terms of stability and hydrolytic activity compared to agarose C8-TLL, and in part this may be related to a different enzyme conformation. Considering that the immobilization conditions define the properties of this enzyme on these kind of supports [79], this result could be expected.

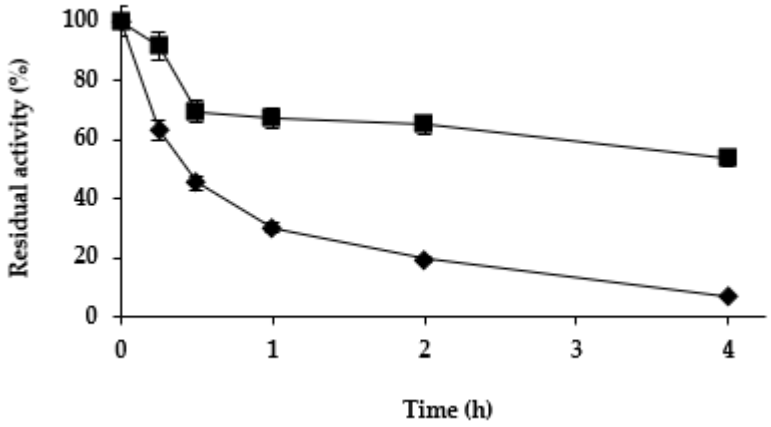

Figure 2. Thermal inactivation courses of agarose C8-TLL and Purolite C18-TLL. Other specifications are described in Methods. Agarose C8-TLL (rhombus) and Purolite C18-TLL (squares).

Next, we intended to further improve these enzyme features via the mineralization of Purolite C18-TLL [61–64].

2.2. Mineralization of Purolite C18-TLL

The biocatalyst was incubated with sodium phosphate and different metal chloride salts to achieve metal phosphate mineralization of the immobilized enzymes [61–64]. Figure 3 shows the color that the biocatalyst acquired after mineralization. The supports were not transparent like agarose, and they initially had a slightly grey color, so the zinc phosphate mineralization does not produce an obvious change in the color. Copper (blue) and cobalt (slight pink) phosphates' mineralization produced an obvious change in the color of the biocatalyst.

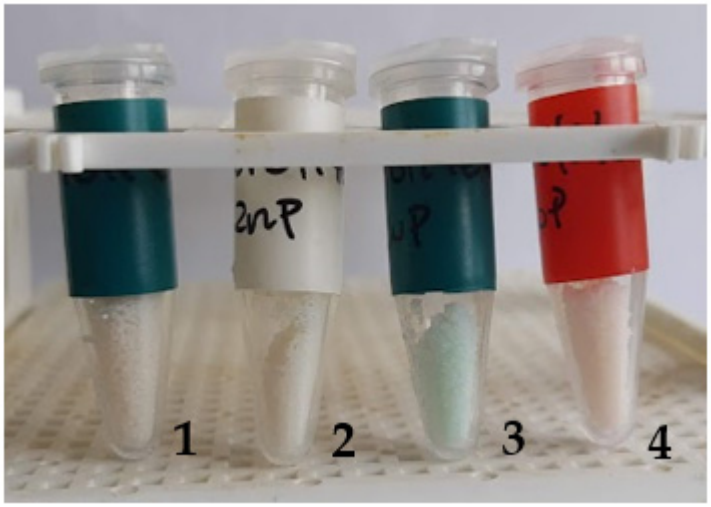

Figure 3. Purolite C18-TLL (1) unmodified, modified with (2) $ZnCl_2$/sodium phosphate, (3) $CuCl_2$/sodium phosphate, and (4) $CoCl_2$/sodium phosphate. Other specifications are described in Methods.

2.2.1. Effect of the Mineralization on Enzyme Hydrolytic Activities

Using agarose C8-TLL [61] and diverse blocked agarose C8-vinyl sulfone-TLL [63], the mineralization greatly affected the enzyme properties, just as with using the commercial TLL biocatalyst [64]. Table 2 shows the hydrolytic activity of the differently modified biocatalysts. When the Purolite C18 biocatalyst was mineralized with zinc phosphate, its hydrolytic activity versus triacetin increased by 23.2%. Due to the high hydrolytic activity of the biocatalysts, it is possible that the effects may be even higher but masked due to substrate diffusion limitations [80–82] and pH gradients [4,83–86]. The same treatment increased the hydrolytic activity of the agarose C8-TLL by around 38.9%, but its activity was still less than a quarter of the activity of the Purolite C18-TLL. The modification with copper salt increased the hydrolytic activity of Purolite C18-TLL similarly to the zinc salt; while using agarose C8-TLL, this treatment produced no change in the hydrolytic activity with this substrate. Cobalt salt mineralization produced the most active biocatalyst, almost 720 U/g, using Purolite C18-TLL (which demonstrated an increase in the hydrolytic activity by 30.5%), while a minor increase in hydrolytic activity was found using agarose C8-TLL (3.2%). These changes in hydrolytic activity suggest that the different mineralizations acting on different enzyme conformations can produce very different effects. For this substrate, the changes are more positive using Purolite C18-TLL than agarose C8-TLL, even though both biocatalysts were based on the same immobilization procedure: lipase interfacial activation [68].

Table 2. Relative activity (calculated as the ratio activity of the modified biocatalyst/activity of the unmodified biocatalysts in percentage) of different TLL-based biocatalysts in the reaction of substrate hydrolysis under the defined conditions. Experiments were conducted as described in Methods.

Biocatalysts	Relative Activity (%)								
	$Zn_3(PO_4)_2$ Modification			$Cu_3(PO_4)_2$ Modification			$Co_3(PO_4)_2$ Modification		
	Triacetin	*R*-Mandelate	*S*-Mandelate	Triacetin	*R*-Mandelate	*S*-Mandelate	Triacetin	*R*-Mandelate	*S*-Mandelate
Agarose C8-TLL	138.9 ± 6.7	69.2 ± 3.9	71.4 ± 2.8	100.0 ± 5.1	100.0 ± 3.4	71.4 ± 4.3	103.2 ± 4.2	69.2 ± 3.5	100.0 ± 5.1
Purolite C18-TLL	123.2 ± 3.7	114.0 ± 5.1	66.7 ± 2.5	120.2 ± 3.6	114.0 ± 4.4	33.3 ± 1.6	130.5 ± 3.9	109.1 ± 6.1	66.7 ± 2.9

For the methyl mandelate isomers, the situation is again different for Purolite C18-TLL and agarose C8-TLL. Focusing on the *R*-isomer, the zinc salt treatment increased the hydrolytic activity of Purolite C18-TLL by 14.0% (while using agarose C8-TLL this activity

decreased to 69.2%); the copper salt treatment produced a similar increase in hydrolytic activity of Purolite C18-TLL while this activity was maintained using agarose C8-TLL, and the cobalt phosphate treatment produced an increase in hydrolytic activity of 9.1% using Purolite C18-TLL, while it decreased to 69.2% using the other biocatalyst. Using the *S*-isomer, all mineralizations decreased the hydrolytic activity of both biocatalysts, but the decrease is much more significant using Purolite C18-TLL (to 33.3% using copper salt) than the agarose C8-TLL (to 71.4% using zinc or copper salts). Thus, while the initial Purolite C18-TLL biocatalyst presented a ratio of activities in hydrolysis of R- to S-enantiomers of 7.3, all mineralizations increased this ratio: using zinc salt, this ratio was 12.5, using copper salt, it was 25, and using cobalt salt, this ratio was 12. For agarose C8-TLL, the changes in this ratio were smaller and some were negative, moving from the initial 1.85 to 1.8, 2,6, or 1.5, respectively.

Thus, the effects of the mineralization of immobilized TLL hydrolytic activity and specificity strongly depended on the support. These results suggest that the enzyme not only had different initial conformation in both biocatalysts, but that the changes induced by the mineralization were also different [59–64].

2.2.2. Effect of the Mineralization on Enzyme Stability

Next, we studied the effect of the different treatments on the stability of the Purolite C18-TLL. In the previous study using agarose C8 beads [61], zinc salt treatment was found to be stabilizing, while cobalt and copper salt treatments slightly destabilized the enzyme. Figure 4 shows that while copper and cobalt salt treatments produced a destabilization of the enzyme (more relevant than using agarose C8-TLL), the zinc salt treatment produced some stabilization. This stabilization was smaller than the one described using agarose C8-TLL [61]. However, as showed in Figure 5, the stability of agarose C8-TLL-zinc phosphate was slightly lower than that of Purolite C18-TLL-zinc phosphate. Thus, the enzyme mineralization effect on enzyme stability depends on the metal used, and also on the utilized support. The higher stabilization caused by the mineralization of agarose C8-TLL greatly decreased the large difference in the initial stability when compared to Purolite C18-TLL.

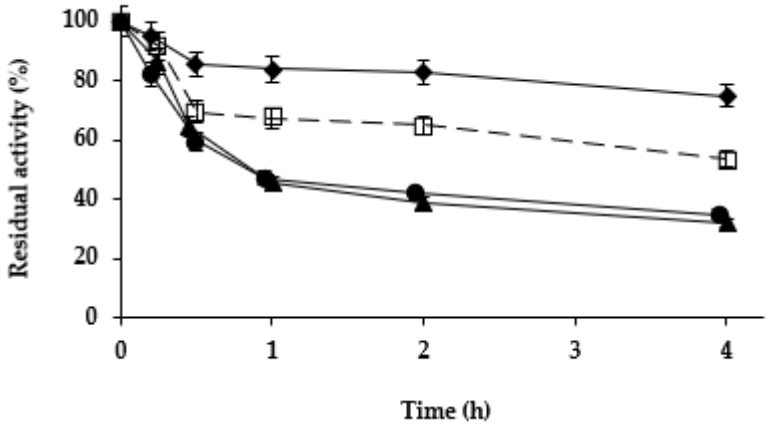

Figure 4. Thermal inactivation courses of different Purolite C18-TLL biocatalysts. Other specifications are described in Methods. Unmodified biocatalyst (open squares and dotted line); biocatalyst modified with $ZnCl_2$/sodium phosphate (solid rhombus and solid line); $CoCl_2$/sodium phosphate (solid triangles and solid line); $CuCl_2$/sodium phosphate (solid circles and solid line).

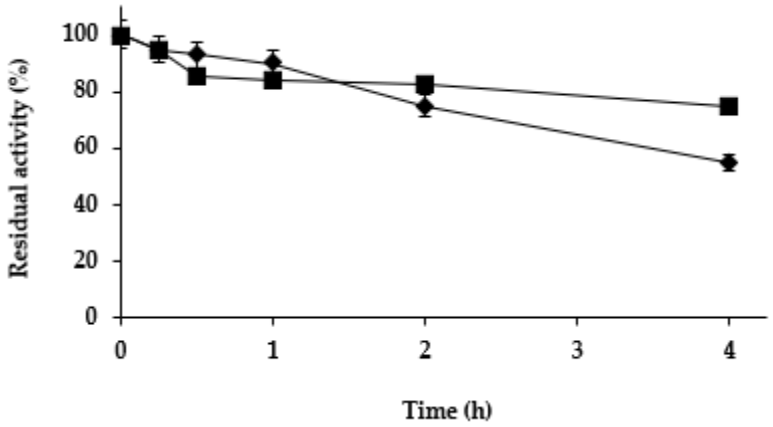

Figure 5. Thermal inactivation courses of agarose C8-TLL-ZnP (rhombus) and Purolite C18-TLL-ZnP (squares). Other specifications are described in Methods.

3. Materials and Methods

3.1. Materials

A TLL solution (20.77 mg protein/mL) was kindly donated by Novozymes Spain (Madrid, Spain). Bradford's reagent (utilized to calculate the protein concentration [87]), *p*-nitrophenyl-butyrate (*p*-NPB), triacetin, *R*- and *S*-methyl mandelate, triacetin, acetonitrile for HPLC (gradient grade, ≥99.9%), cobalt chloride ($CoCl_2$), copper chloride ($CuCl_2$), and zinc chloride ($ZnCl_2$) were purchased from Sigma-Aldrich (St. Louis, MO, USA). Purolite Lifetech® ECR8806F (methacrylate macroporous resin containing octadecyl groups) (Purolite C18) with an average porous diameter of 38.5 nm under dried conditions [88] was kindly donated by Purolite® Ltd. (Wales, UK). Octyl Sepharose® CL-4B (agarose C8) was acquired from GE Healthcare (Uppsala, Sweden), presenting an average porous dimeter of 153 nm in wet conditions [74]. All other reagents were of analytical grade.

3.2. Methods

The experiments were repeated 3 times, and the values are given as mean values and standard deviation.

3.2.1. Wetting of Purolite C18 Beads

1 g of Purolite C18 beads was added to 5 mL of methanol and mildly stirred to eliminate the air inside the particles [75]. After 1 h, 5 mL of distilled water was added, maintaining the stirring for 15 min. Next, the suspensions were submitted to 10 washes (20 volumes each) with distilled water utilizing a vacuum filter, and stowed at 4–6 °C.

3.2.2. Immobilization of TLL

Agarose C8 or hydrated Purolite C18 beads were utilized to immobilize TLL, offering 20 mg of protein per g of support. This is over the support loading capacity [88], but they was utilized to guarantee the full lipase coating of the support surface. The immobilization was initialized mixing 100 mL of enzyme solution in 5 mM sodium phosphate at pH 7.0 and 10 g of the support (that means that the enzyme concentration during the immobilization was 2 mg/mL); the immobilization suspension was maintained at room temperature under gentle stirring. The hydrolytic activity in supernatant and reference was periodically determined using *p*-NPB assay activity. After 2 h, the immobilization suspensions were vacuum filtered, washed 10 times with 20 volumes of distilled water, and kept at 4–6 °C.

3.2.3. Modification of Immobilized Enzymes with Metal Salt/Sodium Phosphate

The immobilized enzymes were mineralized mixing $CoCl_2$, $CuCl_2$ or $ZnCl_2$ and sodium phosphate, as described by Guimarães et al. [61]. The biocatalysts (0.5 g) were suspended in 5 mL of 10 mM sodium phosphate/125 mM NaCl at pH 7.4, and then a

volume of 400 µL of metal salt solution (230 mM) was added and kept at room temperature under mild stirring. After 5 h, the biocatalysts were vacuum filtered, washed 10 times with distilled water (20 volumes each), and stowed at 4–6 °C.

3.2.4. Thermal Inactivation of the Different TLL-Based Biocatalysts

The TLL-based biocatalysts were suspended in 10 mM Tris-HCl (1:10 (*w*:*v*) ratio) at pH 7.0 and submitted at 75 °C. To quantify the residual activities, 50 µL of the inactivation suspensions were withdrawn at the desired times. Residual activities were calculated as the hydrolytic activity at the indicated time divided by the initial hydrolytic activity, and this was stated in percentage. Triacetin was utilized to determine the enzyme activity.

3.2.5. Enzyme Hydrolytic Activity Assays

One unit of activity (U) corresponds to the conversion of 1 µmol of substrate per minute under the described conditions.

Hydrolysis of *p*-NPB

50 µL of a solution/suspension enzyme formulation was mixed with 2.5 mL of 25 mM sodium phosphate at pH 7.0 using a thermostat system at 25 °C, under magnetic stirring. 50 µL of 10 mM *p*-NPB dissolved in acetonitrile were added to initialize the reaction. The hydrolyses were performed for 1.5 min. The *p*-nitrophenol released into the medium was quantified using a spectrophotometer. The wave length was 348 nm, as this is the isosbestic point of this compound (ε = 5150 M^{-1} cm^{-1}) [89].

Hydrolysis of Triacetin

3 mL of 50 mM triacetin was prepared in 50 mM of sodium phosphate at pH 7.0. To initialize the reaction, 50 mg of immobilized enzyme was added at 25 °C under gentle stirring. The degree of hydrolysis was quantified by determining the released 1,2 and 1,3 diacetin (the produced 1,2 diacetin undergoes acyl migration giving 1,3 diacetin at pH 7 [90]) in the reaction medium. A Waters 486 chromatograph (Waters, Millford, MA, USA) presenting a Kromasil C18 column (15 cm × 0.46 cm, EKA Chemicals AB, Bohus, Sweden) and a UV/VIS detector (set to 230 nm) were utilized to follow the degree of conversion (we utilized at least two points, one over 5% and other under 25%). The mobile phase was composed of 85% (*v*/*v*) water and 15% (*v*/*v*) acetonitrile. The flow rate was 1 mL/min. The retention times were 4 min for 1,2 and 1,3 diacetins (they coeluted under these conditions) and 18 min for triacetin [91].

Hydrolysis of *R*- or *S*-Methyl Mandelate

3 mL of 50 mM *R*- or *S*-methyl mandelate was prepared in 50 mM sodium phosphate solution at pH 7.0. To start the reaction, 50 mg of TLL-based biocatalysts were added, maintaining the suspension under gentle stirring at 25 °C. The hydrolysis degree was determined by quantifying the released mandelic acid. A Waters 486 chromatograph (Waters, Millford, MA, USA) with a Kromasil C18 column (15 cm × 0.46 cm, EKA Chemicals AB, Bohus, Sweden) and a UV/VIS detector (set to 230 nm) was employed in the analyses to determine the degree of hydrolysis (two points over 5% and under 25%) [92]. At mobile phase, 65% (*v*/*v*) 10 mM ammonium acetate/35% (*v*/*v*) acetonitrile at pH 2.8 were utilized. The flow rate was set at 1 mL/min. The retention times were 2.5 min for mandelic acid and 4.2 min for methyl mandelate [93]. Activities ratio was defined as the activity versus the *R*-isomer/activity versus the *S*-isomer.

4. Conclusions

The immobilization of TLL on Purolite C18 produced a biocatalyst with properties quite different to those obtained utilizing agarose C8, suggesting that the enzyme structure may be quite different. Purolite C18-TLL was almost inactive in the hydrolysis of *p*-NPB, while it was much more active in the hydrolysis of other substrates (triacetin or methyl

mandelate) than the agarose C8 biocatalyst. Moreover, Purolite C18-TLL presented a higher hydrolytic activity with *R*–methyl mandelate.

The mineralization of Purolite C18-TLL also produced diverse effects compared to the mineralization of agarose C8-TLL. In terms of hydrolytic activity, it was generally more positive with Purolite C18-TLL than with the agarose biocatalyst. However, Purolite C18-TLL lost more stability using cobalt or copper phosphate treatment than using agarose C8-TLL, while its stability increased to a smaller degree using zinc salt treatment.

Therefore, the results suggest that even having an enzyme immobilized using the same protocol (interfacial activation), the differences in the support can generate different enzyme conformations, and thus the enzyme mineralization can present diverse effects on enzyme features. Only after analyzing the mineralization effects on the exact process we can assure that the changes may be positive or negative. Only an empiric analysis can show the effects.

Author Contributions: J.R.G.: Conceptualization, methodology, investigation, visualization, formal analysis, writing—review & editing. D.C.: Investigation, visualization, formal analysis, writing—review & editing. J.R.-M.: Formal analysis, writing—review & editing. P.W.T.: Resources, conceptualization, writing—review & editing, supervision, R.F.-L.: Resources, conceptualization, methodology, writing—original draft, review & editing, supervision. All authors have read and agreed to the published version of the manuscript.

Funding: This research was funded by Coordenação de Aperfeiçoamento de Pessoal de Nível Superior–Brasil (CAPES, Finance Code 001; CAPES-PRINT, Process Number 88887.571985/2020-00), MCIN/AEI/10.13039/501100011033 (PID2021-122398OB-I00). DC thanks to Ministerio de Ciencia e Innovación-Spanish Government by a FPI.

Data Availability Statement: Data can be obtained from the authors.

Acknowledgments: The help and suggestions from Ángel Berenguer (Departamento de Química Inorgánica, Universidad de Alicante) are gratefully recognized. Martinez (Novozymes®, Madrid, Spain) is gratefully recognized for the donation of the enzymes. Basso (Purolite®, Wales, UK) is gratefully recognized for the donation of the supports.

Conflicts of Interest: The authors declare no conflict of interest.

References

1. Fernandez-Lafuente, R. Lipase from *Thermomyces lanuginosus*: Uses and prospects as an industrial biocatalyst. *J. Mol. Catal. B Enzym.* **2010**, *62*, 197–212. [CrossRef]
2. Barbosa, O.; Ortiz, C.; Berenguer-Murcia, Á.; Torres, R.; Rodrigues, R.C.; Fernandez-Lafuente, R. Strategies for the one-step immobilization-purification of enzymes as industrial biocatalysts. *Biotechnol. Adv.* **2015**, *33*, 435–456. [CrossRef] [PubMed]
3. Rodrigues, R.C.; Berenguer-Murcia, Á.; Carballares, D.; Morellon-Sterling, R.; Fernandez-Lafuente, R. Stabilization of enzymes via immobilization: Multipoint covalent attachment and other stabilization strategies. *Biotechnol. Adv.* **2021**, *52*, 107821. [CrossRef] [PubMed]
4. Rodrigues, R.C.; Ortiz, C.; Berenguer-Murcia, Á.; Torres, R.; Fernández-Lafuente, R. Modifying enzyme activity and selectivity by immobilization. *Chem. Soc. Rev.* **2013**, *42*, 6290–6307. [CrossRef]
5. Sheldon, R.A.; van Pelt, S. Enzyme immobilisation in biocatalysis: Why, what and how. *Chem. Soc. Rev.* **2013**, *42*, 6223–6235. [CrossRef]
6. Guisan, J.M.; Fernandez-Lorente, G.; Rocha-Martin, J.; Moreno-Gamero, D. Enzyme immobilization strategies for the design of robust and efficient biocatalysts. *Curr. Opin. Green Sustain. Chem.* **2022**, *35*, 100593. [CrossRef]
7. Bié, J.; Sepodes, B.; Fernandes, P.C.B.; Ribeiro, M.H.L. Enzyme immobilization and co-immobilization: Main framework, advances and some applications. *Processes* **2022**, *10*, 494. [CrossRef]
8. Almeida, F.L.C.; Prata, A.S.; Forte, M.B.S. Enzyme immobilization: What have we learned in the past five years? *Biofuels Bioprod. Biorefining* **2022**, *16*, 587–608. [CrossRef]
9. Garcia-Galan, C.; Berenguer-Murcia, Á.; Fernandez-Lafuente, R.; Rodrigues, R.C. Potential of different enzyme immobilization strategies to improve enzyme performance. *Adv. Synth. Catal.* **2011**, *353*, 2885–2904. [CrossRef]
10. Mateo, C.; Palomo, J.M.; Fernandez-Lorente, G.; Guisan, J.M.; Fernandez-Lafuente, R. Improvement of enzyme activity, stability and selectivity via immobilization techniques. *Enzyme Microb. Technol.* **2007**, *40*, 1451–1463.
11. Bolivar, J.M.; Woodley, J.M.; Fernandez-Lafuente, R. Is enzyme immobilization a mature discipline? Some critical considerations to capitalize on the benefits of immobilization. *Chem. Soc. Rev.* **2022**, *51*, 6251–6290. [CrossRef] [PubMed]

12. Virgen-Ortíz, J.J.; dos Santos, J.C.S.; Berenguer-Murcia, Á.; Barbosa, O.; Rodrigues, R.C.; Fernandez-Lafuente, R. Polyethylenimine: A very useful ionic polymer in the design of immobilized enzyme biocatalysts. *J. Mater. Chem. B* **2017**, *5*, 7461–7490. [CrossRef] [PubMed]
13. Müller, F.; Torger, B.; Allertz, P.J.; Jähnichen, K.; Keßler, S.; Müller, M.; Simon, F.; Salchert, K.; Mäurer, H.; Pospiech, D. Multifunctional crosslinkable itaconic acid copolymers for enzyme immobilization. *Eur. Polym. J.* **2018**, *102*, 47–55. [CrossRef]
14. Poliak, A.; Blumenfeld, H.; Wax, M.; Baughn, R.L.; Whitesides, G.M. Enzyme immobilization by condensation copolymerization into cross-linked polyacrylamide gels. *J. Am. Chem. Soc.* **1980**, *102*, 6324–6336. [CrossRef]
15. Shakeri, F.; Ariaeenejad, S.; Ghollasi, M.; Motamedi, E. Synthesis of two novel bio-based hydrogels using sodium alginate and chitosan and their proficiency in physical immobilization of enzymes. *Sci. Rep.* **2022**, *12*, 2072. [CrossRef] [PubMed]
16. Alnadari, F.; Xue, Y.; Alsubhi, N.H.; Alamoudi, S.A.; Alwabli, A.S.; Al-Quwaie, D.A.; Saud Hamed, Y.; Muhammad Nasiru, M.; Ebrahim, A.A.M.; El-Saadony, M.T.; et al. Reusability of immobilized β-glucosidase on sodium alginate-coated magnetic nanoparticles and high productivity applications. *J. Saudi Chem. Soc.* **2022**, *26*, 101517. [CrossRef]
17. Zhang, W.; Ye, W.; Wang, Y.; Yan, Y. Microfluidic fabrication of tunable alginate-based microfibers for the stable immobilization of enzymes. *Biotechnol. J.* **2022**, *17*, 2200098. [CrossRef]
18. Vasilescu, C.; Paul, C.; Marc, S.; Hulka, I.; Péter, F. Development of a tailored sol-gel immobilized biocatalyst for sustainable synthesis of the food aroma ester n-amyl caproate in continuous solventless system. *Foods* **2022**, *11*, 2485. [CrossRef]
19. Ficanha, A.M.M.; Oro, C.E.D.; Franceschi, E.; Dallago, R.M.; Mignoni, M.L. Evaluation of different ionic liquids as additives in the immobilization of lipase CALB by sol-gel technique. *Appl. Biochem. Biotechnol.* **2021**, *193*, 2162–2181. [CrossRef]
20. Fernandez Caresani, J.R.; Dallegrave, A.; dos Santos, J.H.Z. Amylases immobilization by sol–gel entrapment: Application for starch hydrolysis. *J. Sol-Gel Sci. Technol.* **2020**, *94*, 229–240. [CrossRef]
21. Jegan Roy, J.; Emilia Abraham, T. Strategies in making cross-linked enzyme crystals. *Chem. Rev.* **2004**, *104*, 3705–3722. [CrossRef] [PubMed]
22. Zelinski, T.; Waldmann, H. Cross-linked enzyme crystals (CLECs): Efficient and stable biocatalysts for preparative organic chemistry. *Angew. Chem. (Int. Ed. English)* **1997**, *36*, 722–724. [CrossRef]
23. Staar, M.; Henke, S.; Blankenfeldt, W.; Schallmey, A. Biocatalytically active and stable cross-linked enzyme crystals of halohydrin dehalogenase HheG by protein engineering. *ChemCatChem* **2022**, *14*, e202200145. [CrossRef]
24. Cao, L.; Van Rantwijk, F.; Sheldon, R.A. Cross-linked enzyme aggregates: A simple and effective method for the immobilization of penicillin acylase. *Org. Lett.* **2000**, *2*, 1361–1364. [CrossRef] [PubMed]
25. Schoevaart, R.; Wolbers, M.W.; Golubovic, M.; Ottens, M.; Kieboom, A.P.G.; van Rantwijk, F.; van der Wielen, L.A.M.; Sheldon, R.A. Preparation, optimization, and structures of cross-linked enzyme aggregates (CLEAs). *Biotechnol. Bioeng.* **2004**, *87*, 754–762. [CrossRef] [PubMed]
26. Sheldon, R.A. Characteristic features and biotechnological applications of cross-linked enzyme aggregates (CLEAs). *Appl. Microbiol. Biotechnol.* **2011**, *92*, 467–477. [CrossRef] [PubMed]
27. Sampaio, C.S.; Angelotti, J.A.F.; Fernandez-Lafuente, R.; Hirata, D.B. Lipase immobilization via cross-linked enzyme aggregates: Problems and prospects—A review. *Int. J. Biol. Macromol.* **2022**, *215*, 434–449. [CrossRef]
28. Kreiner, M.; Parker, M.-C. Protein-coated microcrystals for use in organic solvents: Application to oxidoreductases. *Biotechnol. Lett.* **2005**, *27*, 1571–1577. [CrossRef]
29. Monteiro, R.R.C.; dos Santos, J.C.S.; Alcántara, A.R.; Fernandez-Lafuente, R. Enzyme-coated micro-crystals: An almost forgotten but very simple and elegant immobilization strategy. *Catalysts* **2020**, *10*, 891. [CrossRef]
30. Kreiner, M.; Parker, M.C. High-activity biocatalysts in organic media: Solid-state buffers as the immobilisation matrix for protein-coated microcrystals. *Biotechnol. Bioeng.* **2004**, *87*, 24–33. [CrossRef]
31. Gao, J.; Yin, L.; Feng, K.; Zhou, L.; Ma, L.; He, Y.; Wang, L.; Jiang, Y. Lipase immobilization through the combination of bioimprinting and cross-linked protein-coated microcrystal technology for biodiesel production. *Ind. Eng. Chem. Res.* **2016**, *55*, 11037–11043. [CrossRef]
32. Ge, J.; Lei, J.; Zare, R.N. Protein–inorganic hybrid nanoflowers. *Nat. Nanotechnol.* **2012**, *7*, 428–432. [CrossRef] [PubMed]
33. Wang, Z.; Zhang, Y.; Ju, E.; Liu, Z.; Cao, F.; Chen, Z.; Ren, J.; Qu, X. Biomimetic nanoflowers by self-assembly of nanozymes to induce intracellular oxidative damage against hypoxic tumors. *Nat. Commun.* **2018**, *9*, 3334. [CrossRef] [PubMed]
34. Zhu, G.; Hu, R.; Zhao, Z.; Chen, Z.; Zhang, X.; Tan, W. Noncanonical self-assembly of multifunctional DNA nanoflowers for biomedical applications. *J. Am. Chem. Soc.* **2013**, *135*, 16438–16445. [CrossRef] [PubMed]
35. Wilson, L.; Betancor, L.; Fernández-Lorente, G.; Fuentes, M.; Hidalgo, A.; Guisán, J.M.; Pessela, B.C.C.; Fernández-Lafuente, R. Cross-linked aggregates of multimeric enzymes: A simple and efficient methodology to stabilize their quaternary structure. *Biomacromolecules* **2004**, *5*, 814–817. [CrossRef] [PubMed]
36. Du, Y.; Jia, X.; Zhong, L.; Jiao, Y.; Zhang, Z.; Wang, Z.; Feng, Y.; Bilal, M.; Cui, J.; Jia, S. Metal-organic frameworks with different dimensionalities: An ideal host platform for enzyme@MOF composites. *Coord. Chem. Rev.* **2022**, *454*, 214327. [CrossRef]
37. Li, J.; Yin, L.; Wang, Z.; Jing, Y.; Jiang, Z.; Ding, Y.; Wang, H. Enzyme-immobilized metal-organic frameworks: From preparation to application. *Chem.-An Asian J.* **2022**, *17*, e202200751. [CrossRef]
38. Lian, X.; Fang, Y.; Joseph, E.; Wang, Q.; Li, J.; Banerjee, S.; Lollar, C.; Wang, X.; Zhou, H.-C. Enzyme–MOF (metal–organic framework) composites. *Chem. Soc. Rev.* **2017**, *46*, 3386–3401. [CrossRef]

39. Mehta, J.; Bhardwaj, N.; Bhardwaj, S.K.; Kim, K.-H.; Deep, A. Recent advances in enzyme immobilization techniques: Metal-organic frameworks as novel substrates. *Coord. Chem. Rev.* **2016**, *322*, 30–40. [CrossRef]
40. Mohammadi-Mahani, H.; Badoei-dalfard, A.; Karami, Z. Synthesis and characterization of cross-linked lipase-metal hybrid nanoflowers on graphene oxide with increasing the enzymatic stability and reusability. *Biochem. Eng. J.* **2021**, *172*, 108038. [CrossRef]
41. Escobar, S.; Velasco-Lozano, S.; Lu, C.-H.; Lin, Y.-F.; Mesa, M.; Bernal, C.; López-Gallego, F. Understanding the functional properties of bio-inorganic nanoflowers as biocatalysts by deciphering the metal-binding sites of enzymes. *J. Mater. Chem. B* **2017**, *5*, 4478–4486. [CrossRef] [PubMed]
42. Zhang, B.; Li, P.; Zhang, H.; Wang, H.; Li, X.; Tian, L.; Ali, N.; Ali, Z.; Zhang, Q. Preparation of lipase/Zn3(PO4)2 hybrid nanoflower and its catalytic performance as an immobilized enzyme. *Chem. Eng. J.* **2016**, *291*, 287–297. [CrossRef]
43. Lee, S.W.; Cheon, S.A.; Kim, M., II; Park, T.J. Organic–inorganic hybrid nanoflowers: Types, characteristics, and future prospects. *J. Nanobiotechnol.* **2015**, *13*, 54. [CrossRef] [PubMed]
44. Liu, Y.; Shao, X.; Kong, D.; Li, G.; Li, Q. Immobilization of thermophilic lipase in inorganic hybrid nanoflower through biomimetic mineralization. *Colloids Surf. B Biointerfaces* **2021**, *197*, 111450. [CrossRef]
45. Li, C.; Zhao, J.; Zhang, Z.; Jiang, Y.Y.; Bilal, M.; Jiang, Y.Y.; Jia, S.; Cui, J. Self-assembly of activated lipase hybrid nanoflowers with superior activity and enhanced stability. *Biochem. Eng. J.* **2020**, *158*, 107582. [CrossRef]
46. Zhang, Y.; Sun, W.; Elfeky, N.M.; Wang, Y.; Zhao, D.; Zhou, H.; Wang, J.; Bao, Y. Self-assembly of lipase hybrid nanoflowers with bifunctional Ca^{2+} for improved activity and stability. *Enzyme Microb. Technol.* **2020**, *132*, 109408. [CrossRef]
47. Xu, L.; Yu, J.; Wang, A.; Zuo, C.; Li, H.; Chen, X.; Pei, X.; Zhang, P. Efficient synthesis of vitamin A palmitate in nonaqueous medium using self-assembled lipase TLL@apatite hybrid nanoflowers by mimetic biomineralization. *Green Chem. Lett. Rev.* **2018**, *11*, 476–483. [CrossRef]
48. Soni, S.; Dwivedee, B.P.; Banerjee, U.C. An ultrafast sonochemical strategy to synthesize lipase-manganese phosphate hybrid nanoflowers with promoted biocatalytic performance in the kinetic resolution of β-aryloxyalcohols. *ChemNanoMat* **2018**, *4*, 1007–1020. [CrossRef]
49. Lee, H.R.; Chung, M.; Kim, M., II; Ha, S.H. Preparation of glutaraldehyde-treated lipase-inorganic hybrid nanoflowers and their catalytic performance as immobilized enzymes. *Enzyme Microb. Technol.* **2017**, *105*, 24–29. [CrossRef]
50. Cui, J.; Zhao, Y.; Liu, R.; Zhong, C.; Jia, S. Surfactant-activated lipase hybrid nanoflowers with enhanced enzymatic performance. *Sci. Rep.* **2016**, *6*, 27928. [CrossRef]
51. Gao, J.; Kong, W.; Zhou, L.; He, Y.; Ma, L.; Wang, Y.; Yin, L.; Jiang, Y. Monodisperse core-shell magnetic organosilica nanoflowers with radial wrinkle for lipase immobilization. *Chem. Eng. J.* **2017**, *309*, 70–79. [CrossRef]
52. Badoei-dalfard, A.; Monemi, F.; Hassanshahian, M. One-pot synthesis and biochemical characterization of a magnetic collagenase nanoflower and evaluation of its biotechnological applications. *Colloids Surf. B Biointerfaces* **2022**, *211*, 112302. [CrossRef] [PubMed]
53. Qamar, S.A.; Qamar, M.; Bilal, M.; Bharagava, R.N.; Ferreira, L.F.R.; Sher, F.; Iqbal, H.M.N. Cellulose-deconstruction potential of nano-biocatalytic systems: A strategic drive from designing to sustainable applications of immobilized cellulases. *Int. J. Biol. Macromol.* **2021**, *185*, 1–19. [CrossRef] [PubMed]
54. Zhang, M.; Zhang, Y.; Yang, C.; Ma, C.; Tang, J. Enzyme-inorganic hybrid nanoflowers: Classification, synthesis, functionalization and potential applications. *Chem. Eng. J.* **2021**, *415*, 129075. [CrossRef]
55. Alhayali, N.I.; Özpozan, N.K.; Dayan, S.; Özdemir, N.; Yılmaz, B.S. Catalase/Fe_3O_4@Cu^{2+} hybrid biocatalytic nanoflowers fabrication and efficiency in the reduction of organic pollutants. *Polyhedron* **2021**, *194*, 114888. [CrossRef]
56. Zhaoyu, Z.; Ping, X.; Keren, S.; Weiwei, Z.; Chunmiao, H.; Peng, L. Di-functional magnetic nanoflowers: A highly efficient support for immobilizing penicillin G acylase. *J. Chin. Chem. Soc.* **2020**, *67*, 1591–1601. [CrossRef]
57. Feng, N.; Zhang, H.; Li, Y.; Liu, Y.; Xu, L.; Wang, Y.; Fei, X.; Tian, J. A novel catalytic material for hydrolyzing cow's milk allergenic proteins: Papain-$Cu_3(PO_4)_2$·3H2O-magnetic nanoflowers. *Food Chem.* **2020**, *311*, 125911. [CrossRef]
58. Sun, T.; Fu, M.; Xing, J.; Ge, Z. Magnetic nanoparticles encapsulated laccase nanoflowers: Evaluation of enzymatic activity and reusability for degradation of malachite green. *Water Sci. Technol.* **2020**, *81*, 29–39. [CrossRef]
59. Zhang, H.; Fei, X.; Tian, J.; Li, Y.; Zhi, H.; Wang, K.; Xu, L.; Wang, Y. Synthesis and continuous catalytic application of alkaline protease nanoflowers–PVA composite hydrogel. *Catal. Commun.* **2018**, *116*, 5–9. [CrossRef]
60. Sun, B.; Wang, Z.; Wang, X.; Qiu, M.; Zhang, Z.; Wang, Z.; Cui, J.; Jia, S. Paper-based biosensor based on phenylalanine ammonia lyase hybrid nanoflowers for urinary phenylalanine measurement. *Int. J. Biol. Macromol.* **2021**, *166*, 601–610. [CrossRef]
61. Guimarães, J.R.; Carballares, D.; Rocha-Martin, J.; Tardioli, P.W.; Fernandez-Lafuente, R. Stabilization of immobilized lipases by treatment with metallic phosphate salts. *Int. J. Biol. Macromol.* **2022**, *213*, 43–54. [CrossRef] [PubMed]
62. Guimarães, J.R.; Carballares, D.; Tardioli, P.W.; Rocha-Martin, J.; Fernandez-Lafuente, R. Tuning immobilized commercial lipase preparations features by simple treatment with metallic phosphate salts. *Molecules* **2022**, *27*, 4486. [CrossRef] [PubMed]
63. Guimarães, J.R.; Carballares, D.; Rocha-martin, J.R.; Tardioli, P.W.; Fernandez-Lafuente, R. The immobilization protocol greatly alters the effects of metal phosphate modification on the activity/stability of immobilized lipases. *Int. J. Biol. Macromol.* **2022**, *222*, 2452–2466. [CrossRef] [PubMed]
64. Guimarães, J.R.; Carballares, D.; Rocha-martin, J.; Tardioli, P.W.; Fernandez–Lafuente, R. Tuning immobilized enzyme features by combining solid-phase physicochemical modification and mineralization. *Int. J. Mol. Sci.* **2022**, *23*, 12808. [CrossRef] [PubMed]

65. Kaur, H.; Bari, N.K.; Garg, A.; Sinha, S. Protein morphology drives the structure and catalytic activity of bio-inorganic hybrids. *Int. J. Biol. Macromol.* **2021**, *176*, 106–116. [CrossRef]
66. Carpenter, B.P.; Talosig, A.R.; Mulvey, J.T.; Merham, J.G.; Esquivel, J.; Rose, B.; Ogata, A.F.; Fishman, D.A.; Patterson, J.P. Role of molecular modification and protein folding in the nucleation and growth of protein–metal–organic frameworks. *Chem. Mater.* **2022**, *34*, 8336–8344. [CrossRef]
67. Manoel, E.A.; dos Santos, J.C.S.; Freire, D.M.G.; Rueda, N.; Fernandez-Lafuente, R. Immobilization of lipases on hydrophobic supports involves the open form of the enzyme. *Enzyme Microb. Technol.* **2015**, *71*, 53–57. [CrossRef]
68. Rodrigues, R.C.; Virgen-Ortíz, J.J.; dos Santos, J.C.S.; Berenguer-Murcia, Á.; Alcantara, A.R.; Barbosa, O.; Ortiz, C.; Fernandez-Lafuente, R. Immobilization of lipases on hydrophobic supports: Immobilization mechanism, advantages, problems, and solutions. *Biotechnol. Adv.* **2019**, *37*, 746–770. [CrossRef]
69. Fernandez-Lorente, G.; Cabrera, Z.; Godoy, C.; Fernandez-Lafuente, R.; Palomo, J.M.; Guisan, J.M. Interfacially activated lipases against hydrophobic supports: Effect of the support nature on the biocatalytic properties. *Process Biochem.* **2008**, *43*, 1061–1067. [CrossRef]
70. Tacias-Pascacio, V.G.; Peirce, S.; Torrestiana-Sanchez, B.; Yates, M.; Rosales-Quintero, A.; Virgen-Ortíz, J.J.; Fernandez-Lafuente, R. Evaluation of different commercial hydrophobic supports for the immobilization of lipases: Tuning their stability, activity and specificity. *RSC Adv.* **2016**, *6*, 100281–100294. [CrossRef]
71. Cunha, A.G.; Besteti, M.D.; Manoel, E.A.; Da Silva, A.A.T.; Almeida, R.V.; Simas, A.B.C.; Fernandez-Lafuente, R.; Pinto, J.C.; Freire, D.M.G. Preparation of core-shell polymer supports to immobilize lipase B from *Candida antarctica*: Effect of the support nature on catalytic properties. *J. Mol. Catal. B Enzym.* **2014**, *100*, 59–67. [CrossRef]
72. Manoel, E.A.; Pinto, M.; dos Santos, J.C.S.; Tacias-Pascacio, V.G.; Freire, D.M.G.; Pinto, J.C.; Fernandez-Lafuente, R. Design of a core–shell support to improve lipase features by immobilization. *RSC Adv.* **2016**, *6*, 62814–62824. [CrossRef]
73. Cipolatti, E.P.; Pinto, M.C.C.; Robert, J.d.M.; da Silva, T.P.; Beralto, T.d.C.; Santos, J.G.F.; de Castro, R.d.P.V.; Fernandez-Lafuente, R.; Manoel, E.A.; Pinto, J.C.; et al. Pilot-scale development of core–shell polymer supports for the immobilization of recombinant lipase B from *Candida antarctica* and their application in the production of ethyl esters from residual fatty acids. *J. Appl. Polym. Sci.* **2018**, *135*, 46727. [CrossRef]
74. Zucca, P.; Fernandez-Lafuente, R.; Sanjust, E. Agarose and its derivatives as supports for enzyme immobilization. *Molecules* **2016**, *21*, 1577. [CrossRef]
75. Tacias-Pascacio, V.G.; Virgen-Ortíz, J.J.; Jiménez-Pérez, M.; Yates, M.; Torrestiana-Sanchez, B.; Rosales-Quintero, A.; Fernandez-Lafuente, R. Evaluation of different lipase biocatalysts in the production of biodiesel from used cooking oil: Critical role of the immobilization support. *Fuel* **2017**, *200*, 1–10. [CrossRef]
76. Tacias-Pascacio, V.G.; Torrestiana-Sánchez, B.; Dal Magro, L.; Virgen-Ortíz, J.J.; Suárez-Ruíz, F.J.; Rodrigues, R.C.; Fernandez-Lafuente, R. Comparison of acid, basic and enzymatic catalysis on the production of biodiesel after RSM optimization. *Renew. Energy* **2019**, *135*, 1–9. [CrossRef]
77. Ching-Velasquez, J.; Fernández-Lafuente, R.; Rodrigues, R.C.; Plata, V.; Rosales-Quintero, A.; Torrestiana-Sánchez, B.; Tacias-Pascacio, V.G. Production and characterization of biodiesel from oil of fish waste by enzymatic catalysis. *Renew. Energy* **2020**, *153*, 1346–1354. [CrossRef]
78. Purolite LifetechTM ECR8806M-Metacrilato de Octadecil. Available online: https://www.purolite.com/ls-product/es/ecr8806m (accessed on 6 October 2022).
79. Lokha, Y.; Arana-Peña, S.; Rios, N.S.; Mendez-Sanchez, C.; Gonçalves, L.R.B.B.; Lopez-Gallego, F.; Fernandez-Lafuente, R. Modulating the properties of the lipase from *Thermomyces lanuginosus* immobilized on octyl agarose beads by altering the immobilization conditions. *Enzyme Microb. Technol.* **2020**, *133*, 109461. [CrossRef]
80. AL-Muftah, A.E.; Abu-Reesh, I.M. Effects of internal mass transfer and product inhibition on a simulated immobilized enzyme-catalyzed reactor for lactose hydrolysis. *Biochem. Eng. J.* **2005**, *23*, 139–153. [CrossRef]
81. Bolivar, J.M.; Consolati, T.; Mayr, T.; Nidetzky, B. Quantitating intraparticle O2 gradients in solid supported enzyme immobilizates: Experimental determination of their role in limiting the catalytic effectiveness of immobilized glucose oxidase. *Biotechnol. Bioeng.* **2013**, *110*, 2086–2095. [CrossRef]
82. Berendsen, W.R.; Lapin, A.; Reuss, M. Investigations of reaction kinetics for immobilized enzymes-identification of parameters in the presence of diffusion limitation. *Biotechnol. Prog.* **2008**, *22*, 1305–1312. [CrossRef] [PubMed]
83. Bolivar, J.M.; Nidetzky, B. The microenvironment in immobilized enzymes: Methods of characterization and its role in determining enzyme performance. *Molecules* **2019**, *24*, 3460. [CrossRef] [PubMed]
84. JM, G.; Alvaro, G.; CM, R.; Fernandez-Lafuente, R. Industrial design of enzymic processes catalysed by very active immobilized derivatives: Utilization of diffusional limitations (gradients of pH) as a profitable tool in enzyme engineering. *Biotechnol. Appl. Biochem.* **1994**, *20*, 357–369. [CrossRef] [PubMed]
85. Byers, J.P.; Shah, M.B.; Fournier, R.L.; Varanasi, S. Generation of a pH gradient in an immobilized enzyme system. *Biotechnol. Bioeng.* **1993**, *42*, 410–420. [CrossRef]
86. Chen, G.; Fournier, R.L.; Varanasi, S. A mathematical model for the generation and control of a pH gradient in an immobilized enzyme system involving acid generation. *Biotechnol. Bioeng.* **1998**, *57*, 394–408. [CrossRef]
87. Bradford, M.M. A rapid and sensitive method for the quantitation of microgram quantities of protein utilizing the principle of protein-dye binding. *Anal. Biochem.* **1976**, *72*, 248–254. [CrossRef]

88. Martínez-Sanchez, J.A.; Arana-Peña, S.; Carballares, D.; Yates, M.; Otero, C.; Fernandez-Lafuente, R. Immobilized biocatalysts of Eversa®transform 2.0 and lipase from *Thermomyces lanuginosus*: Comparison of some properties and performance in biodiesel production. *Catalysts* **2020**, *10*, 738. [CrossRef]
89. Lombardo, D.; Guy, O. Effect of alcohols on the hydrolysis catalyzed by human pancreatic carboxylic-ester hydrolase. *Biochim. Biophys. Acta (BBA)-Enzymol.* **1981**, *657*, 425–437. [CrossRef]
90. Hernandez, K.; Garcia-Verdugo, E.; Porcar, R.; Fernandez-Lafuente, R. Hydrolysis of triacetin catalyzed by immobilized lipases: Effect of the immobilization protocol and experimental conditions on diacetin yield. *Enzyme Microb. Technol.* **2011**, *48*, 510–517. [CrossRef]
91. Arana-Peña, S.; Lokha, Y.; Fernández-Lafuente, R. Immobilization on octyl-agarose beads and some catalytic features of commercial preparations of lipase a from *Candida antarctica* (Novocor ADL): Comparison with immobilized lipase B from *Candida antarctica*. *Biotechnol. Prog.* **2019**, *35*, e2735. [CrossRef]
92. Paiva Souza, P.M.; Carballares, D.; Lopez-Carrobles, N.; Gonçalves, L.R.B.; Lopez-Gallego, F.; Rodrigues, S.; Fernandez-Lafuente, R. Enzyme-support interactions and inactivation conditions determine *Thermomyces lanuginosus* lipase inactivation pathways: Functional and florescence studies. *Int. J. Biol. Macromol.* **2021**, *191*, 79–91. [CrossRef]
93. dos Santos, J.C.S.; Rueda, N.; Gonçalves, L.R.B.; Fernandez-Lafuente, R. Tuning the catalytic properties of lipases immobilized on divinylsulfone activated agarose by altering its nanoenvironment. *Enzyme Microb. Technol.* **2015**, *77*, 1–7. [CrossRef]